SETAC PRESS

Environmental Toxicology and Chemistry, Vol. 23, No. 10, pp. 2324–2336, 2004

Printed in the USA
0730-7268/04 $12.00 + .00

Special Issue Honoring Don Mackay

INTESTINAL ABSORPTION AND BIOMAGNIFICATION OF ORGANIC CONTAMINANTS IN FISH, WILDLIFE, AND HUMANS

BARRY C. KELLY,† FRANK A.P.C. GOBAS,*† and MICHAEL S. MCLACHLAN‡
†School of Resource and Environmental Management, Simon Fraser University, Burnaby, British Columbia V5A 1S6, Canada
‡Institute of Applied Environmental Research, Stockholm University, SE-106 91 Stockholm, Sweden

(*Received* 8 *October* 2003; *Accepted* 11 *March* 2004)

Abstract—Methods for the regulatory assessment of the bioaccumulation potential of organic chemicals are founded on empirical measurements and mechanistic models of dietary absorption and biomagnification. This study includes a review of the current state of knowledge regarding mechanisms and models of intestinal absorption and biomagnification of organic chemicals in organisms of aquatic and terrestrial food chains and also includes a discussion of the implications of these models for assessing the bioaccumulation potential of organic chemicals. Four mechanistic models, including biomass conversion, digestion or gastrointestinal magnification, micelle-mediated diffusion, and fat-flush diffusion, are evaluated. The models contain many similarities and represent an evolution in understanding of chemical bioaccumulation processes. An important difference between the biomagnification models is whether intestinal absorption of an ingested contaminant occurs solely via passive molecular diffusion through serial resistances or via facilitated diffusion that incorporates an additional advective transport mechanism in parallel (i.e., molecular ferrying within gastrointestinal micelles). This difference has an effect on the selection of physicochemical properties that best anticipate the bioaccumulative potential of commercial chemicals in aquatic and terrestrial food chains. Current regulatory initiatives utilizing K_{OW} threshold criteria to assess chemical bioaccumulation potential are shown to be unable to identify certain bioaccumulative substances in air-breathing animals. We urge further research on dietary absorption and biomagnification of organic chemicals to develop better models for assessing the bioaccumulative nature of organic chemicals.

Keywords—Persistent organic pollutants Intestinal absorption Biomagnification Mechanisms Models

INTRODUCTION

Emissions of persistent organic chemicals are widely recognized to result in ubiquitous dispersal in local and global environments and bioaccumulation in organisms. Equilibrium partitioning of a dispersed chemical causes bioconcentration into organism lipids via passive molecular diffusion. Bioconcentration factors (BCFs), the ratios of a chemical's equilibrium concentration in an organism (C_B, wet-wt basis) and that in the organism's respired media (C_R; i.e., BCF = C_B/C_R), are largely dependent on an organism's lipid content. However, equilibrium concentrations of hydrophobic chemicals (expressed on a lipid-wt basis) will be equivalent among different organisms, regardless of lipid content. In addition to bioconcentration, some organic contaminants such as polychlorinated biphenyls (PCBs) and DDT also are known to biomagnify, resulting in chemical concentrations (on a lipid-wt basis) in an organism (C_B) that exceed concentrations in consumed prey (C_D) [1–7]. Concentration-based biomagnification factors (BMFs) are typically reported on a lipid-weight basis ($BMF_C = C_B/C_D$, lipid wt). Bioaccumulation factors (i.e., BAF = C_B/C_R), represent bioconcentration plus biomagnification. Food-chain biomagnification occurs when lipid-weight concentrations increase with increasing trophic position (TP; i.e., $C_{TP,4} > C_{TP,3} > C_{TP,2} > C_{TP,1}$). These bioaccumulative substances are of great concern because of their potential to attain toxicologically significant tissue and organ residue concentrations in high-trophic-level species such as predatory fish, birds, and mammals (including humans) [8–10]. The DDT-induced eggshell thinning in birds of prey such as the peregrine falcon (*Falco peregrinus*) during the 1960s is perhaps the most notorious example of the potential deleterious effects of bioaccumulative substances [8,11].

To avoid the perils of bioaccumulative substances such as DDT and PCBs, governments in Canada, the United States, and Europe have launched proactive and preventative measures to reduce or eliminate similar future risks from current-use and proposal-stage chemicals of commerce. For example, Canada has adopted a Toxic Substances Management Policy under the Canadian Environmental Protection Act in accordance with the recent Stockholm Convention on persistent organic pollutants (POPs) [12]. This policy considers virtual elimination of chemicals that meet criteria for persistence, bioaccumulation, and inherent toxicity. Current bioaccumulation criteria identify ''bioaccumulative'' substances as those compounds that exhibit BAFs or BCFs greater than 5,000 in aquatic organisms, or (in the absence of BAF or BCF data) chemicals with octanol–water partition coefficients (K_{OW}s) greater than 10^5. The K_{OW} threshold criterion is a marker of bioaccumulation potential in aquatic organisms because of the mechanistic understanding that chemicals with $K_{OW}s < 10^5$ may bioconcentrate in aquatic organisms (i.e., accumulate from water via the organism's respiratory surface such as gills) but do not biomagnify because of efficient clearance of chemical to water via gill ventilation [13–16].

This simple K_{OW}-based structure–activity relationship for bioaccumulation of commercial chemicals was derived from observations and biomagnification models for aquatic organisms [4,14,15,17]. The adoption of this relationship in policies implies that it is also considered to be appropriate for assessing bioaccumulation in numerous other organisms, including birds, reptiles, mammals, and humans. In addition, current mechanistic models may not be appropriate for all organisms

* To whom correspondence may be addressed (gobas@sfu.ca).

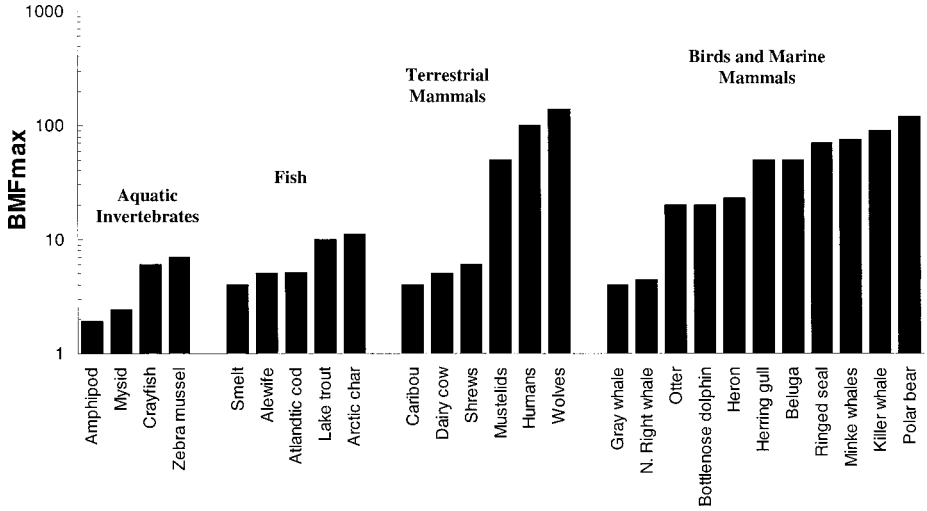

Fig. 1. Reported biomagnification factors (BMF_{MAX}s) of PCB 153 in organisms from various freshwater, terrestrial, and marine ecosystems. The BMF_{MAX} values represent lipid-equivalent or lipid-normalized concentration-based BMFs (C_B/C_D lipid). References for BMF data are: amphipods [5]; mysids, smelt, and alewife [18]; crayfish, zebra mussels, and lake trout [15]; Atlantic cod and ringed seals [33]; Arctic char, beluga whales, and polar bears [26]; caribou and wolves [7]; dairy cows [20]; shrews [21]; mustelids and otters [25]; humans [32]; gray whales [31]; North Atlantic right whales [30]; bottlenose dolphins [27]; Baikal seals [29]; herons [24]; herring gulls [22,23]; minke whales [28]; and killer whales [10]. White bars represent invertebrates, light gray bars represent fish, dark gray bars represent terrestrial mammals, and black bars represent marine mammals.

or for all classes of compounds. For example, as is illustrated in Figure 1, the magnitude of the BMF_C (lipid wt) of stable nonmetabolizable compounds (e.g., PCB 153) varies by orders of magnitude among different classes of organisms. Reported BMFs of PCB 153 typically range between 5 and10 for invertebrates and fish [5,14–16,18]; 5 and 10 for caribou, dairy cows, and shrews [7,19–21]; 20 and 60 for birds [22–24]; 30 and 40 for mustelids [25]; and approach 100 or greater for marine mammals [10,26–31], wolves [7], and humans [32]. Investigations of POPs in the Great Lakes by Norstrom and colleagues [22] highlighted that BMFs of organochlorines in Lake Ontario herring gulls were approximately 10 times higher than those BMFs in Lake Ontario coho salmon. Numerous other studies have documented this interspecies variability in BMFs between aquatic poikilotherms (invertebrates and fish) and homeotherms (birds and mammals) [2,6,33]. Consequently, utilization of observed BMFs in aquatic organisms as a surrogate for bioaccumulation potential can substantially underestimate the extent of chemical biomagnification in birds and mammals. Also, some relatively hydrophilic compounds such as β-hexachlorocyclohexane, α-endosulfan, and chlorobenzenes (log K_{OW}s range from 3.8 to 4.5) have shown considerable biomagnification in air-breathing organisms (i.e., birds and mammals), whereas they are not known to biomagnify in aquatic organisms [5,7,33,34]. Another example is perfluorooctane sulfonate, which is a water-soluble, nonvolatile anionic compound. This substance does not meet the current K_{OW} criterion for bioaccumulative substances and does not biomagnify in fish [35]. However, perfluorooctane sulfonate is efficiently absorbed via dietary exposures, biomagnifies and persists in the liver and blood of air-breathing animals [36–39], and is inherently toxic [40,41]. Modeling studies of POP bioaccumulation in arctic caribou and wolves [42] have demonstrated that relatively hydrophilic (i.e., polar, $K_{OW}s < 10^5$) but nonvolatile compounds (i.e., octanol–air partition coefficients [K_{OA}s] $> 10^5$) that are resistant to metabolism (half-life $>$ 60 d) biomagnify because of efficient gastrointestinal absorption and very slow lipid-to-air elimination via respired air. This emerging evidence indicates that the current K_{OW}-based classification of chemicals is not an adequate model to identify substances with a bioaccumulative potential in food webs that include mammals, birds, and humans. The significance of this issue is emphasized by the fact that approximately two thirds of the chemical substances used commercially in Canada have been indicated as having possible bioaccumulative potential in birds and mammals (including humans). Of these substances, about half are polar nonvolatile compounds with low K_{OW}s (i.e., log $K_{OW}s < 5$), whose bioaccumulation potential may be miscategorized [43]. These chemicals include many chemicals of concern such as flame retardants, surfactants, pesticides, plasticizers, fluorinated and alkylphenol ethoxylates, pharmaceuticals, sunscreen agents, and synthetic fragrances [44].

To develop better and more proactive policies for identifying bioaccumulative substances, it is important to better characterize the dominant underlying processes and mechanisms driving the biomagnification phenomenon. These processes include dietary absorption, various elimination processes, metabolic transformation, and growth dilution. In this paper, we will review the current thinking on dietary absorption and biomagnification of organic substances. Several research groups recently have made significant contributions in this area. The objectives of our paper are first to review the current state of knowledge of mechanisms and models of intestinal absorption and bioaccumulation of organic chemicals in wildlife and humans and second to discuss the implications of these models for assessing the bioaccumulative potential of organic substances. Specifically, we outline and evaluate four different intestinal absorption and biomagnification mechanisms and models. It is our hope that this discussion will lead to the formulation of better models to assess the biomagnification behavior of organic chemicals in food webs.

THEORY

The fugacity approach

In this study we use the fugacity approach to formulate models for dietary absorption and biomagnification. Mackay

and colleagues [45,46] have previously demonstrated the benefits of using chemical fugacity to describe and quantify chemical transport in environmental systems and food webs. The fugacity of a chemical (f, pascals [Pa]) for a given phase is related linearly to its molar concentration (C, mol/m^3) by the fugacity capacity (Z, mol/m^3/Pa) of the phase in which the chemical is solubilized

$$f = C/Z \quad (1)$$

The fugacity capacity is compound and phase specific and represents the ability of that phase to sorb and retain a given chemical within its matrix. In essence, the fugacity is a measure of the chemical's concentration normalized to the chemical's solubility in the medium it resides in. The ratio of the fugacity capacities (Z) of two adjacent media or compartments i and j (i.e., Zi/Zj) can be viewed as a partition coefficient K_{ij}, which is equivalent to Ci/Cj at equilibrium. Thus, $K_{OW} = Z_O/Z_W = C_O/C_W$, whereas $K_{OA} = Z_O/Z_A = C_O/C_A$.

In the fugacity approach, chemical uptake and clearance processes occur via advection, diffusion, or reaction (e.g., metabolism). In the fugacity format, transport of chemical for these processes is described in terms of transport parameters (or D values, mol/Pa/d), which are related to concentration-based rate constants (k, d^{-1}). Relatively large values represent fast processes, whereas small D values indicate slower processes. If transport of chemicals between different media is diffusive in nature, D can be determined from the chemical's molecular diffusivity (B, m^2/d), the surface area of diffusion (A, m^2), the Z of the phase, and the length of the diffusion path (d, m)

$$D_{DIFFUSION} = (BAZ)/d \quad (2)$$

Diffusive processes between phases or compartments are reversible and the D value for diffusion from medium i to j is equal to that from medium to j to i. The diffusive flux (denoted as N, mol/d) between media or compartments can be described by

$$N = D(f_i - f_j) \quad (3)$$

where the term $(f_i - f_j)$ represents the departure from equilibrium or driving force between two phases (i.e., media) or compartments i and j. If chemical fugacities are not equal, the direction of chemical flow occurs from the high-fugacity compartment to the low-fugacity compartment. If chemical fugacities become equal, the two compartments have attained a chemical equilibrium and the chemical flux (N) is zero. If the transport process is advective in nature, the transport parameter D is the product of a flow rate (G, m^3/d) of a given medium and Z, mol/m^3/Pa, of the chemical in the advective medium

$$D_{ADVECTION} = GZ \quad (4)$$

Advective transport processes between phases or compartments are unidirectional and in cases where a distribution is the result of advective inflows and outflows, the net flux (denoted as N, mol/d) between media or compartments can be described by

$$N = D_i f_i - D_j f_j \quad (5)$$

Equation 5 demonstrates that transport will take place until $D_i f_i$ equals $D_j f_j$, at which $N = 0$ (i.e., steady state) and the fugacities $f_i/f_j = D_i/D_j$. If chemical is generated or depurated by a chemical reaction (e.g., metabolism), the D value is related to the first-order rate constant (k), the compartment volume (V, m^3), and the Z of the phase

$$D_{METABOLISM} = VkZ \quad (6)$$

The D values are equivalent to conductivities for chemical mass. Hence, their reciprocal ($1/D$) can be viewed as a resistance to the mass transport a chemical encounters in a given phase. If transport and reaction processes occur in series, the reciprocal D values add to give the total resistance to chemical transport

$$1/D_{TOTAL} = 1/D_1 + 1/D_2 + 1/D_3 + \ldots \quad (7)$$

If chemical transport and transformation occur in parallel, D values are additive

$$D_{TOTAL} = D_1 + D_2 + D_3 + \ldots \quad (8)$$

The ability to add serial resistances or parallel transport parameters is convenient for quantifying chemical transfer in biological systems due to the presence of multiple, simultaneously occurring processes, resistance pathways, or both.

In fugacity terms, biomagnification in the food chain is defined as a state where fugacities increase with increasing trophic level (e.g., $f_{VEGETATION} < f_{HERBIVORE} < f_{CARNIVORE}$). The purpose of this paper is to explore the underlying mechanism of this phenomenon and to explore how this mechanism can be formalized in a fugacity-based model that is useful for bioaccumulation assessment.

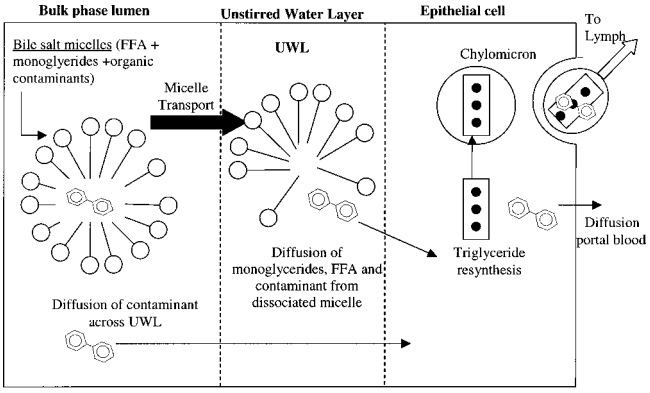

Fig. 2. Schematic illustration of gastrointestinal uptake of dietary fats and xenobiotics. The illustration is modified from Sanford [47]. UWL = unstirred water layer; FFA = free fatty acid.

Intestinal absorption of xenobiotic molecules

Numerous reviews of lipid absorption and digestive physiology have been conducted [47–51]. Figure 2 depicts the transcellular migration path of dietary fats and environmental contaminants (i.e., xenobiotics) from lumen across the epithelium of the gut wall. The formation of mixed micelles from bile salt molecules in the gastrointestinal tract (GIT) and their function with respect to lipid digestion is well documented [48–51]. The purpose of bile salt micelles in the GIT is twofold. The first is to remove monoglycerides and free fatty acids from the vicinity of digesting fat globules so the digestion process can proceed unabated and the second is to act as a transport medium by ferrying monoglycerides, free fatty acids, fat-soluble vitamins A, D, and K, and thus consequently hydrophobic organic contaminants across an unstirred water layer (UWL) to the luminal membrane. This stagnant water layer is estimated to be approximately 0.05 to 2 mm thick in humans

and is relatively more acidic (pH between 5.1 and 6.3) than the aqueous phase of the intestinal contents. The greater acidity aids the diffusion of fatty acids across the membrane by increasing the fraction of the un-ionized free fatty acid in the aqueous phase. A pH decrease within the UWL adjacent to the brush border membrane (BBM) is believed to cause dissociation of the micelles, which then results in fatty acids and xenobiotics (e.g., PCBs) separating from the micelles and permeating through the water phase into the BBM of the epithelial cells as monomers [49]. However, some evidence suggests that collisional contact of mixed micelles and intestinal cell membranes causes release of lipids and chemical directly into the BBM [50]. The significance of the latter process is that it would essentially eliminate the resistance to membrane transfer posed by the aqueous diffusion barrier adjacent to the BBM and bypass diffusion altogether. Molecules in the intestine can be transported across the epithelium of the gut by either a transcellular route (across the plasma membrane of the epithelial cells) or by a paracellular route (across tight junctions between epithelial cells). Although water and polar organic compounds may be transported by both routes, the tight junctions are generally impermeable to large nonpolar organic molecules (e.g., fats and PCBs with minimal internal cross sections > 1 Å). Hence, those molecules are transported exclusively by the transcellular route [47]. Beyond the BBM in the cytosol, the absorbed digestion products (i.e., fatty acids and monoglycerides) are resynthesized into triglycerides, which are subsequently packaged with phospholipids and apoproteins to form lipid vesicles (referred to as lipoproteins or chylomicrons). The lipid vesicles then migrate to the basolateral membranes where they are released by exocytosis into lymph, venous blood, or both. Compounds absorbed directly in the cytosol (individual molecules) can then either diffuse directly across the basolateral membrane into portal blood or become solubilized in lipoproteins and subsequently released via exocytosis. Dulfer et al. [52] recently formalized the above transcellular migration path of organic chemicals in terms of chemical fugacities and transport parameters (D values) for the various intestinal components [see Fig. S-1 in SETAC Supplemental Data Archive, Item ETC-23-10-001; http://etc.allenpress.com].

MECHANISMS OF BIOMAGNIFICATION

Biomass conversion model

The first mechanistic explanation of the biomagnification phenomenon was documented by Woodwell [1] based on the observed increase in concentrations of PCBs and DDT in biota with increase in trophic level in a marine aquatic food web. Woodwell reasoned that PCBs and DDTs were efficiently ingested and absorbed in association with food but depurated at a rate slower than the consumption of biomass needed for energy requirements. In fugacity terms, this process can be formulated as

$$N_B = V_B Z_B df_B/dt = D_D f_D - D_E f_B \quad (9)$$

where N_B is the net absorption of chemical by the organism (i.e., $V_B Z_B df_B/dt$), $D_D f_D$ is the rate of chemical absorption (mol/d) via dietary ingestion, $D_E f_B$ is the rate of chemical depuration (mol/d) via all possible routes, D_D is the transport parameter of chemical absorption via dietary ingestion (mol/d/Pa), f_D is the chemical fugacity in the diet, D_E is the transport parameter for chemical depuration (mol/d/Pa), f_B is the chemical fugacity in the organism, V_B is the volume, Z_B is the fugacity capacity of the organism, and t is time. At steady state ($N_B = 0$), Equation 9 becomes $f_B/f_D = D_D/D_E$, which demonstrates that biomagnification can occur for chemicals for which $D_E < D_D$.

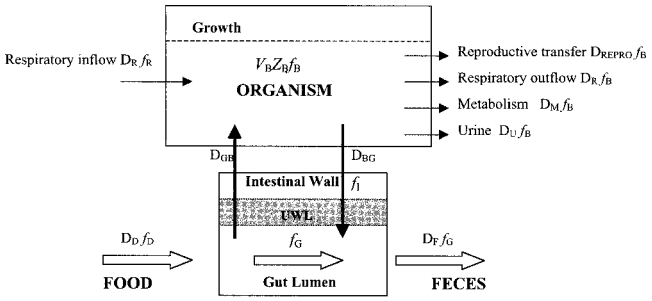

Fig. 3. Conceptual illustration of a two-compartment model of uptake and elimination of organic chemicals in a generic water-ventilating or air-respiring organism. The gastrointestinal tract compartment (denoted as subscript G) is shown to include the intestinal wall (denoted as subscript I), separated by an unstirred water layer (UWL).

One of the characteristics of this mechanism is that chemical is moved from a low fugacity in the prey to a high fugacity in the predator. This constitutes a mass transport against the thermodynamic gradient, which indicates that ingested chemical is predominantly absorbed via a nondiffusive active transport process. A second feature of this mechanism is that the magnification of the chemical concentration occurs as a result of energy consumption in the tissues of the organism. The latter has led to the application of bioenergetic models to estimate the degree of chemical magnification [53].

Digestion model

Hydrophobic organic chemicals as well as monoglycerides and fatty acids are ideally suited to diffuse through and pass biological membranes because of their lipophilicity [54] and hence do not require an active transport mechanism for absorption. To explain the apparent transport of hydrophobic organic chemicals against the thermodynamic gradient, it was hypothesized that organic chemicals are magnified in the GIT of organisms as a result of food digestion [13,55,56]. In this mechanism, the chemical concentration and fugacity in the GIT of an organism are increased as food is absorbed. In essence, digestion of consumed food in the GIT concentrates ingested chemical residues in a reduced and compositionally altered digesta matrix, which causes a fugacity pump or gastrointestinal magnification (i.e., f_G exceeds f_D). This creates a positive thermodynamic gradient between the GIT and the organism (i.e., $f_G > f_B$). This gradient is required for net passive absorption of chemical. If elimination by excretion or metabolism is negligible, the chemical concentration and fugacity in the organism will increase to match that in the GIT. The latter will cause the concentration in the organism to exceed that in its food.

This mechanism can be formalized in fugacity terms in a two-compartment model, consisting of a GIT with a volume V_G (m^3) and an organism compartment with volume V_B (m^3) representing the animal's overall contaminant storage in various tissues and viscera (Fig. 3). To maintain simplicity, the GIT is viewed as a single well-mixed homogenous compartment. Although these simplifications have adequately represented bioaccumulation of POPs in several organisms [14,19,42,46], more complex multicompartment bioaccumulation models can be utilized if tissue- of organ-specific resolution is desired [57,58]. Chemical enters the GIT at a rate of $D_D f_D$, which is equal to the product of the volumetric feeding

rate (G_D, m^3/d), the fugacity capacity of the food (Z_D, mol/Pa/m^3), and the fugacity in the diet (f_D), that is, $G_D Z_D f_D$ or simply $G_D C_D$. Digested food leaves the GIT in fecal matter at a rate of $D_F f_G$, which is equal to the product the fecal egestion rate (G_F, m^3/d), the fugacity capacity of the feces (Z_G), and the fugacity in the fecal matter (f_G), that is, $G_F Z_G f_G$ or simply $G_F C_G$. Chemical moves from the GIT to the organism at a rate of $D_{GB} f_G$. The reverse transport takes place at a rate of $D_{BG} f_B$. The net flux (N_G) into the GIT can therefore be expressed as

$$N_G = V_G Z_G \mathrm{d}f_G/dt = D_D f_D + D_{BG} f_B - (D_F + D_{GB}) f_G \quad (10)$$

The organism compartment, which for reasons of simplicity is also represented as a single well-mixed compartment, receives chemical from contaminant flux between the GIT and organism ($D_{GB} f_G$), and uptake via the respiratory route ($D_R f_R$), that is, uptake from water or air. Chemical depuration (mol/d) can occur through excretion into the digesta ($D_{BG} f_B$) and subsequent fecal excretion, respiratory elimination ($D_R f_R$), urinary excretion ($D_U f_U$), reproductive transfer and lactation ($D_{REPRO} f_B$), and metabolic transformation (D_M, equivalent to $k_M C_B V_B$, where k_M [d^{-1}] is the metabolic transformation rate constant of the chemical in the organism). Growth dilution ($D_B f_B$) caused by an animal's increase in body storage volume (V_B) and lipid content (ν_{LB}) over time essentially dilutes internal chemical concentration (C_B) while increasing storage capacity (i.e., Z_B). Conversely, depletion of an animal's fat reserves concentrates chemical residues while decreasing storage capacity (i.e., Z_B). Growth can be particularly important for nursing newborns, organisms that periodically undergo significant seasonal body condition changes (e.g., hibernating mammals), and physiologically stressed organisms (e.g., diseased animals). The net flux (N_B) into the organism can therefore be expressed as

$$N_B = V_B Z_B \mathrm{d}f_B/dt = D_R f_R + D_{GB} f_G - (D_{BG} + D_R + D_M + D_B + D_U + D_{REPRO}) f_B \quad (11)$$

If it can be assumed that the GIT is at steady state, that is, $N_G = 0$ and $f_G = (D_D f_D + D_{BG} f_B)/(D_{GB} + D_F)$, substitution into Equation 11 yields an interesting expression for the fugacity-based BMF (BMF_f) at steady state

$$BMF_f = f_B/f_D = [D_R + (D_D/D_F)] \times [D_{GB}/(D_{BG} + D_R + D_M + D_B + D_U + D_{REPRO})] \quad (12)$$

This equation demonstrates the role of some of the key factors in controlling the BMF of organic chemicals. The equation demonstrates that food digestion is a key factor in the magnification of the chemical because D_D/D_F, which equals $G_D Z_D/G_F Z_G$ or $G_D/G_F)(Z_D/Z_G)$ will exceed 1 in proportion to the extent to which the fecal excretion rate (G_F) drops below the dietary intake rate (G_D) and to the degree to which the fugacity capacity of the diet (Z_D) is lowered to Z_G as a result absorption of lipids, proteins, and other dietary components. Following a three-phase partitioning model employed by Kelly and Gobas [42], Z_D/Z_G can be derived as

$$Z_D/Z_G = C_B/C_G = K_{DG} = (\nu_{LD} + 0.035 \cdot \nu_{NLD} + \nu_{WD}/K_{OW}) \div (\nu_{LG} + 0.035 \cdot \nu_{NLG} + \nu_{WG}/K_{OW}) \quad (13)$$

where ν_{LD}, ν_{NLD}, and ν_{WD} are the lipid, nonlipid organic matter, and water contents of ingested food (kg/kg wet wt food) and ν_{LG}, ν_{NLG}, and ν_{WG} are the lipid, nonlipid organic matter, and water contents of the gut contents (kg/kg wet wt digesta). Equation 12 also demonstrates the role of metabolic transformation and other mechanisms of elimination. If the exchange of chemical between the GIT and the organism is dominated by passive diffusion, D_{GB} and D_{BG} are equal and the depuration processes combine to drive $D_{GB}/(D_{BG} + D_R + D_M + D_B + D_U + D_{REPRO})$ below 1. In the hypothetical case of a complete absence of depuration routes (i.e., D_R, D_M, D_B, D_U, and D_{REPRO} are all zero), the maximum attainable BMF_f approaches

$$BMF_f = f_B/f_D = D_D/D_F = (G_D/G_F)(Z_D/Z_G) \quad (14)$$

This result is the same as for the biomass conversion model. The essence of the digestion model is that food digestion is the key process responsible for actual magnification of the chemical concentration in the predator. A key assumption of this model is that the exchange of chemical between the GIT and the organism is dominated by passive diffusion (i.e., molecular diffusion is the rate-limiting step in GIT–organism chemical transport). This means that D_{GB} and D_{BG} are equal. The model views micellar transport (D_{MIC}) and subsequent diffusion of the chemical through UWLs (D_W) and the phospholipid bilayers (D_L) as processes applying in series, that is

$$1/D_{GB} = 1/D_{MIC} + 1/D_W + 1/D_L \quad (15)$$

with the slowest step in the chain of events controlling the overall rate of gastrointestinal uptake. As discussed by Gobas and colleagues [59], this implies that dietary absorption rates (e.g., quantified by the gross dietary absorption efficiency [E_D]) can be expected to fall with increasing K_{OW}, because the low aqueous concentrations of highly hydrophobic compounds in the UWLs control the rate of intestinal uptake, that is

$$1/E_D = \alpha K_{OW} + \beta \quad (16)$$

where α and β are organism-specific constants.

Figure 4 is an illustrative example of gastrointestinal magnification model–predicted fugacities (nPa) at steady state of a nonmetabolizable, nonvolatile, and hydrophobic compound such as PCB 153 in an aquatic poikilotherm (e.g., fish) and a

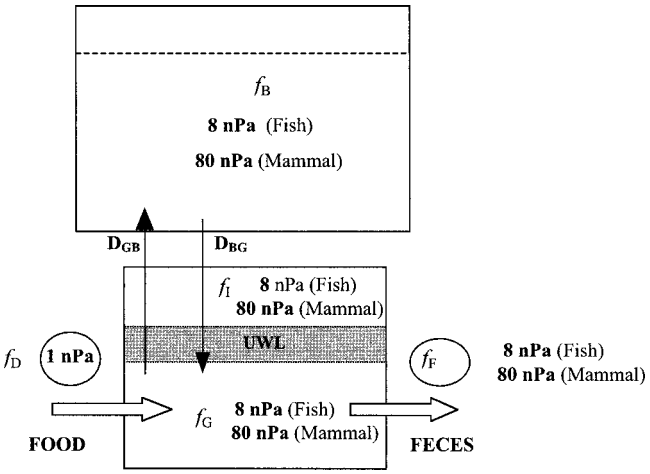

Fig. 4. Steady-state conditions of chemical fugacities in the gastrointestinal tract (GIT) and organism for fish and homeothermic organisms such as birds and mammals following gastrointestinal magnification model. The GIT compartment (denoted as subscript G) is shown to include the intestinal wall (denoted as subscript I), separated by an unstirred water layer (UWL).

Table 1. Summary of physiological parameters, feeding rates, digestion efficiencies, and observed biomagnification factors (BMF_C lipid wt) for fish (poikilotherms) and birds and mammals (homeotherms)[a]

	Rainbow trout[b]	Dairy cow[c]	Caribou[d]	Ring dove[e]	Harp seal[f]	Human[g]	Stellar sea lion[h]	Wolf[i]
Body weight (kg)	0.439	250	140	0.16	57	80	600	90
Whole-body lipid content (%)	3	20	4	17	42	20	40	21
Energetic requirements (% BW/d_g)	1.2	2	2.1	7.7	3.3	1.1	5	2.8
Feeding rate (kg/d)	0.004	4	3	0.01179	1.881	0.9	30	2.5
Lipid content food (%)	18	1	0.05	9.10	8	20	9	12
Fecal egestion rate (kg/d)	0.002	1.6	1.2	0.0039	0.38	0.032	1.80	0.13
Lipid assimilation efficiency (%)	92	60	60	98	94	95	97	98
Food assimilation efficiency (%)	50	60	60	70	80	92	94	95
G_D/G_F	2	2	2.5	3.4	5	13	17	20
Z_D/Z_G[j]	4	2	0.8	5	4	6	6	7
E_{MAX} (%)	60	80	—	97	—	100	—	—
Observed BMF_{MAX} (C_B/C_D lipid wt)	8	4	3	52	23	≥ 80	≥ 100	≥ 100

[a] BW = body weight; G_D = dietary intake rate; G_F = fecal excretion rate; Z_D = fugacity capacity of diet; Z_G = fugacity capacity of feces; E_{MAX} = maximum absorption efficiency; C_B = concentration in organism; C_D = concentration in diet.
[b] Gobas et al. [60].
[c] McLachlan [19, 62].
[d] Kelly and Gobas [42].
[e] Drouillard and Nordstrom [61, 64].
[f] Fraser et al. [65].
[g] Schlummer et al. [32] and Moser [63].
[h] Lee et al. [66] and Rosen and Trites [67].
[i] Kelly et al. [42].
[j] Z_D/Z_G ratios were estimated by using the three-phase partitioning model in Kelly et al. [42].

homeotherm (e.g., mammal). Figure 4 shows a fugacity increase from 1 nPa in consumed food (f_D = 1 nPa) to approximately 8 nPa in the GIT for fish. The eight times fugacity increase in the GIT, due to a G_D/G_F ratio of approximately two (i.e., 50% food absorption) and a Z_D/Z_G ratio of approximately 4 (based on 95% lipid, 60% nonlipid organic matter, and 95% water extraction efficiency), results in a gastrointestinal magnification factor of 2 × 4 or 8 in fish. Thus, the steady-state fugacities for food (f_D), intestinal tissues (f_I), body tissues (f_B), and fecal matter (f_F) in fish are (f_D:f_I:f_B:f_F = 1:8:8:8) under these hypothetical conditions. For homeotherms, Figure 4 shows a fugacity increase from 1 nPa in consumed food (f_D = 1 nPa) to approximately 80 nPa in the GIT. The digestion model explains the comparatively high BMFs observed in homeotherms (e.g., $BMF = f_B/f_D = (G_D/G_F)(Z_D/Z_G) = 80$) compared to fish (e.g., $BMF = (f_B/f_D = (G_D/G_F)(Z_D/Z_G) = 8$) as a result of a greater efficiency of the digestive system. A more efficient digestive system means that organisms exhibit larger G_D/G_F (e.g., 20 based on a 95% food absorption) and Z_D/Z_G (e.g., between 4 and 10, based on a ≥98% lipid, ≥60% nonlipid organic matter, and 95% water extraction efficiency). The magnitude of the decrease in Z also is sensitive to the lipid content of the prey species (i.e., quantity of dietary lipids ingested) [42]. The combined effect of food absorption (G_D/G_F) and extraction of dietary constituents (Z_D/Z_G) will produce greater gastrointestinal magnification factors and BMFs (~80 or greater; i.e., ≥ 10 times greater than the BMF in fish) and a fugacity distribution of f_D:f_I:f_B:f_F = 1:80:80:80. Table 1, which shows a comparison of dietary absorption parameters and BMF_{MAX} values for fish, birds, and terrestrial and marine mammals [19,32,42,60–67], demonstrates that homeothermic carnivores (typically exhibiting a BMF_{MAX} 10–20 times higher than that of fish) tend to consume larger amounts of lipid-rich prey and have a higher degree of lipid and food absorption compared to fish.

Considerable evidence is available for the role of food digestion on dietary absorption and biomagnification. Initial evidence supporting the digestion model comes from experiments [59] in which three batches of fish were fed low fat (LF), medium fat (MF), and high fat (HF) diets. The three diets contained a series of hydrophobic organic chemicals at the same concentration but at varying fugacities (i.e., $f_{LF} > f_{MF} > f_{HF}$, due to $Z_{LF} < Z_{MF} < Z_{HF}$). These authors hypothesized that if molecular diffusion was rate limiting, then GIT–organism chemical uptake rates (N_D, mol/d) and absorption efficiencies (E_D) would increase with decreasing lipid content in the food (because of increased fugacity). Conversely, if micelle-facilitated diffusion was dominating, then increased lipid content should result in higher uptake (N_D) and absorption efficiencies (E_D). The results showed that dietary uptake rates increased with reduced lipids in consumed food because of increased chemical fugacity in the diet. This suggested that the hydrophobic organic chemicals tested (PCBs and chlorobenzenes) were absorbed via passive diffusion and that a positive fugacity gradient between the intestines and the organism is a key determinant for dietary absorption. These authors concluded that lipid vesicle transport (i.e., micelle-facilitated diffusion) was not rate limiting in the GIT–organism flux in the exposed fish because increased lipid ingestion did not result in increased chemical uptake (N_D) or absorption (E_D).

Further evidence to demonstrate that the chemical fugacity in the intestinal tract can be raised over that in the diet came from three sets of laboratory studies with guppies, goldfish, and adult rainbow trout and a comparative field study [17,59,60]. Direct and indirect measurements of the fugacity of a series of hydrophobic organic chemicals in the intestinal content of these fish species showed that fugacities in the diet are increased in the intestines as a result of food digestion. The studies showed that the occurrence of a fugacity pump in the GIT is mainly due to the lipid absorption efficiency (~92% in fish) being greater than the chemical absorption efficiency (i.e., ~75% or less). The fact that lipids are absorbed from the gut lumen at a faster rate than the chemical produces an increase in fugacity in the gut lumen over that in the diet

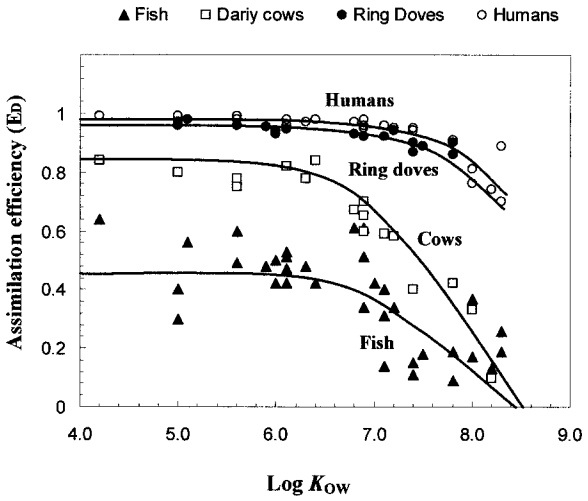

Fig. 5. Dietary absorption efficiencies of various persistent organic pollutants reported in the literature for several organisms, including fish [13], dairy cows [62], humans [63], and ring doves [61] versus chemical log K_{OW}. Trend lines represent nonlinear regressions: $1/E_D = 5.3 \times 10^{-8} K_{OW} + 2.3$ for fish data; $1/E_D = 2.9 \times 10^{-8} K_{OW} + 1.2$ for dairy cows; $1/E_D = 2.4 \times 10^{-9} K_{OW} + 1.04$ for ring doves; and $1/E_D = 1.55 \times 10^{-9} K_{OW} + 1.01$ for human data, where E_D = dietary absorption efficiency.

consumed. The magnitude of the fugacity increase observed in fish (i.e., eight times increase from f_D to f_G) corresponded to a four times decrease from Z_D to Z_G and a two times decrease in digesta volume ($G_D/G_F = 2$).

The relationship between dietary absorption efficiency and chemical K_{OW} has been previously investigated in fish [13,16,59], birds [61], dairy cows [19,62], and humans [32,63]. Examination of data from these comparable studies (plotted in Fig. 5) demonstrates that absorption of ingested chemical in both homeotherms (ring doves, dairy cows, and humans) and an aquatic poikilotherm (fish) shows a tendency to be relatively constant for low-K_{OW} substances, but decreases with increasing K_{OW} (E_D decreases significantly when log $K_{OW} >$ 7). Gobas and colleagues [17,59,60] suggested that the declining trend in E_D in fish is consistent with a diffusion-controlled dietary absorption mechanism, where micellar transport and diffusion through UWLs and diffusion through phospholipid bilayers apply in series. For low-K_{OW} substances, micellar transport, phospholipid bilayer diffusion, or both are the rate-determining steps, whereas diffusion through UWLs is rate limiting for very high–K_{OW} substances with very low solubilities in the water layers. These authors further suggested that if gastrointestinal absorption processes would apply in parallel, then micellar transport should control gastrointestinal uptake of the higher-K_{OW} chemicals and should be similar for all compounds.

Micelle-mediated diffusion model

To explain the higher BMFs in homeotherms compared to aquatic poikilotherms, Drouillard and Norstrom [61] proposed that micelle-mediated diffusion (MMD) can produce a magnification effect in addition to or in place of food digestion. This process involves micelle-facilitated chemical transport from the bulk lumen to the organism (i.e., GIT to organism) through unidirectional advection of mixed micelles across the aqueous resistance of the UWL, whereas the reverse flux (i.e., organism to GIT) is somewhat reduced because micelles become dissociated within an acidic pH microclimate present at the vicinity of the intestinal wall. In essence, the MMD model assumes that intestinal absorption of chemical (enhanced by mixed-micelle facilitation) occurs in the upper GIT in association with dietary lipid absorption, whereas chemical elimination (decoupled in time and space) occurs at a much slower rate in the lower digestive tract. Thus, the mixed-micelle transport in the upper intestine causes the rate of chemical uptake across the UWL into gut tissue to be substantially faster than the rate of reverse diffusion back to the intestine. In fugacity terms, the transport parameter D_{GB} in Equations 11 and 12 is greater than D_{BG}. This results in a sustained fugacity increase in the organism's tissues over that in the intestines and the original diet consumed. These authors proposed that the higher energetic demands of homeothermic animals (birds and mammals) compared to fish result in higher feeding rates in homeothermic animals. The higher feeding rates produce greater mixed-micelle concentrations in the GIT and hence greater chemical uptake rates through direct transfer of the chemical-containing micelles to intestinal tissue. This ultimately causes a high fugacity build up in the animal's tissues due to very slow diffusive elimination rate back to the GIT.

This mechanism was formalized in fugacity format by Cahill et al. [57] by using a physiologically based pharmacokinetic model that incorporates a micelle-mediated uptake mechanism. In their generalized physiologically based pharmacokinetic model designed for evaluating multiresidue toxicokinetics, gastrointestinal uptake is described as a parallel aqueous and MMD. The MMD model assumes that gastrointestinal uptake (D_{GB}) is described as the sum of simultaneous parallel processes including micellar transport (D_{MIC}), direct aqueous diffusion (D_W), and diffusion across the cell membrane (D_{CELL}), as described by Dulfer et al. [52]

$$D_{GB} = D_{MIC} + D_W + D_{CELL} \quad (17)$$

This model of intestinal absorption assumes unidirectional micelle-facilitated diffusion across the UWL followed by molecular diffusion through the cell membrane, whereas aqueous molecular diffusion of contaminant into gut tissue is bidirectional. The primary difference of this model from that of the digestion hypothesis is the assumption of unequal chemical uptake (D_{GB}) and elimination (D_{BG}), specifically that $D_{GB} > D_{BG}$. A D_{GB}/D_{BG} ratio greater than 1 inherently suggests that chemical is more efficiently absorbed from the intestine than it is lost to the intestine. This ratio represents an additional magnification factor to any magnification that may occur as a result of food digestion. The latter is demonstrated by Equation 12, which in the hypothetical case of a complete absence of depuration routes (i.e., D_R, D_M, D_B, D_U, and D_{REPRO} are zero) simplifies to

$$\begin{aligned} BMF_f &= f_B/f_D = (D_D/D_F)(D_{BG}/D_{BG}) \\ &= (G_D/G_F)(Z_D/Z_G)(D_{GB}/D_{BG}) \end{aligned} \quad (18)$$

The MMD model therefore suggests the larger BMFs exhibited by homeotherms compared to aquatic poikilotherms can be explained by a larger D_{GB}/D_{BG} ratio in homeotherms.

Figure 6 illustrates theoretical MMD model–predicted fugacities (nPa) of typical hydrophobic POPs at steady-state in a fish and a homeotherm (e.g., mammal). The disparity in D values across the gut wall is the central distinction of the MMD hypotheses (i.e., $D_{GB} > D_{BG}$). The steady-state fugacities for food (f_D), intestinal tissues (f_I), body tissues (f_B), and fecal

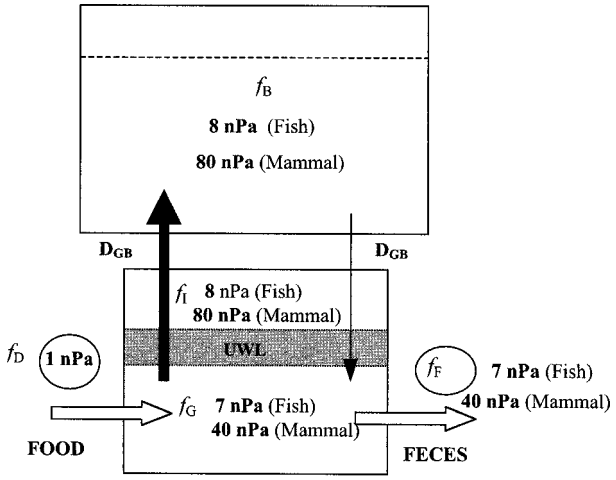

Fig. 6. Steady-state conditions of chemical fugacities in the gastrointestinal tract (GIT) and organism for fish and homeothermic organisms such as birds and mammals following the unidirectional micelle-mediated diffusion model. The GIT compartment (denoted as subscript G) is shown to include the intestinal wall (denoted as subscript I), separated by an unstirred water layer (UWL). Model predictions are based on a mixed-micelle enhancement factor (i.e., D_{GB}/D_{BG} ratio) of approximately 1.2 for fish and 2.0 for birds and mammals.

matter (f_F) are f_D: f_I: f_B: f_F = 1:8:8:7 for fish and f_D: f_I: f_B: f_F = 1:80:80:40 for a mammal.

Numerous studies have provided evidence for the cotransport of organic chemicals with lipid vesicles in the GIT, lymphatic flow, or both [51,68–71]. Vetter et al. [72] used light microscopy to examine intestinal contents and tissues after the absorption of administered benzo[*a*]pyrene in killifish. Their results indicated coassimilation of dietary fats and chemical via lipid vesicles into the BBM and into fat droplets within the enterocytes and that separation of chemical from dietary lipids occurs primarily after lipid absorption and reassembling in the enterocyte. However, other studies of intestinal absorption of benzo[*a*]pyrene suggested that separation of chemical from dietary lipids occurs in the lumen, followed by passive diffusion of single monomers into the enterocyte [73].

The semiempirical fugacity-based cell-line model developed by Dulfer et al. [52] [see Fig. S-1 in SETAC Supplemental Data Archive, Item ETC-23-10-01; http://etc.allenpress.com] provides some empirical evidence of the presence of a micelle-facilitated transport mechanism for hydrophobic contaminants across human intestinal membranes. Specifically, in vitro studies of PCB absorption in human colorectal carcinoma–derived cells (Caco-2 cells) [52] showed that the presence of mixed micelles can increase chemical flux into intestinal cells more than 1,000-fold compared to cell lines without mixed micelles because of the relatively high affinity of hydrophobic organic chemicals for mixed micelles (Z_{MIC}). These authors suggested that micelle-mediated transport of chemical from the upper intestine (gut lumen to intestinal tissue) is likely a substantially faster process than the reverse transport back across the UWL (intestinal tissue to gut lumen) because the latter process is assumed to occur by diffusion alone.

Drouillard and Norstrom [61], in their study of dietary uptake of PCB congeners in ring doves (*Streptopelia risoria*), found dietary absorption efficiencies of PCBs (93–83% over a log K_{OW} range of 5–7.5) were comparable to the lipid absorption efficiency (90%). Furthermore, these authors found that PCB congeners entered blood plasma at similar rates to dietary lipids. These findings suggest that lipids and ingested contaminant are absorbed in association, which indicates that a fugacity pump in the GIT may not occur because the onset of gastrointestinal magnification primarily is caused by a higher rate of lipid removal from the GIT compared to the rate of chemical absorption. These authors observed a small (~10%) decline in absorption efficiencies of PCB in ring doves with increasing K_{OW} (see Fig. 5), which was attributed to solubility limitations of those high-K_{OW} compounds in the nucleus of the interior of the mixed micelles, rather than kinetic limitations across the stagnant aqueous UWL (as is suggested in the digestion model). This argument is supported by measurements of membrane–water partition coefficients (K_{MW}s) for chemicals of varying K_{OW} [74,75], which demonstrate that the solubility of hydrophobic organic chemicals in membrane vesicles increases with increasing K_{OW} up to a maximum K_{OW} value of approximately seven and then decreases with further increasing K_{OW} (see Fig. S-2 in supporting information). In a complimentary depuration study of gavaged PCBs in ring doves, Drouillard and Norstrom [64] reported an approximate 30% decline in excreta–carcass partition coefficient (K_{ExC}; over the log K_{OW} range of 5–7.5). These authors suggested that the more pronounced 30% drop in K_{ExC} during the depuration experiment, compared to the slight 10% drop in absorption efficiencies during the uptake experiments [61], indicates that for the more hydrophobic PCBs gut-to-organism uptake exceeds organism-to-gut transfer (i.e., $D_{GB} > D_{BG}$).

Fat-flush diffusion hypothesis

Schlummer et al. [32] recently presented a fat-flush diffusion (FFD) model for intestinal uptake in humans. This model is based on the premise that the lipid influx into intestinal cells acts to enhance gastrointestinal magnification and diffusive uptake from intestinal contents. These authors postulated that the fugacity capacity of intestinal cells (Z_I) increases during periods of active food digestion, when dietary lipids are hydrolyzed to monoglycerides and fatty acids and subsequently resynthesized into triglycerides in the enterocyte. The fugacity of the reformed triglycerides in intestinal tissues (Z_{TRI}) is greater than that of the monoglycerides or fatty acids originating from the mixed micelles in the lumen (Z_{MIC}) [52,71], which thereby enhances the diffusion gradient from the lumen into the intestine. The resulting lipid swelling in the enterocyte causes a downward pressure on the fugacity in the intestinal cells because f_I is inversely proportional to Z_I. At the same time, the fugacity in the gut lumen (i.e., GIT) is increased as Z_G decreases as a result of lipid transfer from the lumen to the intestinal cells. This effect produces a positive fugacity gradient between the gut lumen and the intestinal cells resulting in net absorption. Although the fat-flush effect has only been formalized to assess human dietary exposures, it is likely to also occur in other organisms (especially those that digest large quantities of lipids, such as top-predator carnivores). Because previous fugacity measurements in dietary accumulation studies with fish by Gobas and colleagues [17,59,60] indicated the fat flush does not occur in fish, we will confine the following evaluation of the FFD model to humans.

Figure 7 illustrates the fat-flush effect over the course of a digestion event. At the time of ingestion, f_D (1 nPa) is lower than f_I (80 nPa). As food digestion and absorption ensues, f_G increases and f_I decreases simultaneously, allowing for net passive diffusion of chemical into the intestinal tissue (subscript I). During the rapid period of efficient lipid absorption

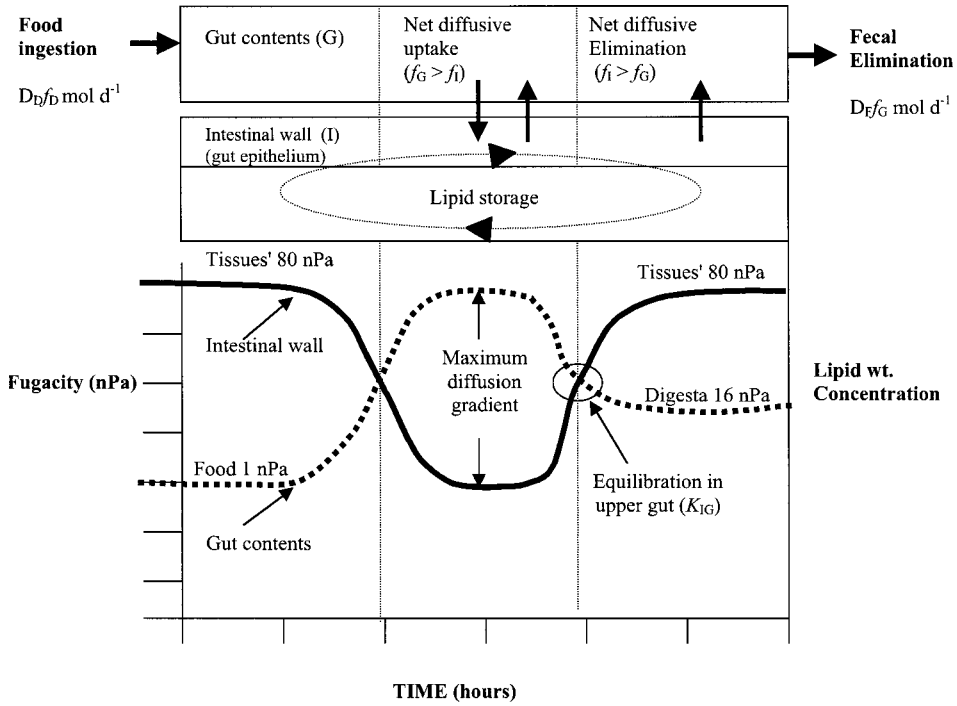

Fig. 7. Schematic illustration of the fat-flush hypothesis, modified from Schlummer et al. [32]

and chylomicron transport of resynthesized triglycerides, a subsequent removal of chemical from the digesta occurs in the GIT (causing f_G to decrease as digestion proceeds). Equilibrium partitioning between the digesta and intestinal tissue continues over the 2- to 4-h period of digesta transit in the upper gut until a partitioning equilibrium between the intestinal tissues and digesta is achieved (e.g., f_G is shown to equilibrate with f_I at 16 nPa). Absorbed lipids and chemical are transported from intestinal tissue to the liver, and eventually an equilibrium within the body is restored (f_I increases to 80 nPa). Simultaneously, the digesta (f_G = 16 nPa) is advectively transported into the lower digestive tract during the later stages of the digestion event and diffusive elimination back to the feces becomes possible because f_I (80 nPa) > f_F (16 nPa). In essence, the absorption of dietary lipids simultaneously causes a fugacity increase in the digesta moving through the upper intestine and simultaneously an influx of lipid pools in the BBM, which in effect increases the Z of the intestinal tissue (resulting in a temporary fugacity decrease in intestinal tissue). The combined effect of the high fugacity in the gut contents (f_G) and the reduced fugacity in the intestinal tissue (f_I) facilitates efficient chemical absorption due to the temporary thermodynamic gradient. The fugacity in the lower digestive tract (i.e., feces) is only indirectly influenced by the fat flush, because the fat flush has subsided by the time the digesta arrive there.

Figure 8a further examines the FFD model predictions of a human subject from the general population, exhibiting POP tissue residue levels approximately 80 times that of consumed food (i.e., f_B/f_D = BMF_f = 80). Specifically, the fugacity in the diet at 1 nPa may attain approximately a 16-fold fugacity increase in the upper gut (i.e., f_G = 16 nPa) because of food absorption and digestion (i.e., gastrointestinal magnification), and a simultaneous five times or greater increase in the fugacity capacity of intestinal tissue Z_I, which causes the fugacity in the intestinal tissues to decrease. The diffusive gradient from the digesta into the intestinal tissue results and chemical is taken up (i.e., net uptake occurs) until a partitioning equilibrium between the digesta and the intestinal tissue is achieved (e.g., f_D:f_G:f_I:f_B = 1:16:16:80). Consequently, in the lower digestive tract, the fugacity in the digesta is considerably lower than in the intestinal tissue (i.e., f_B:f_I:f_G = 80:80:16). Based on the findings of Rozman et al. [76], which indicated that contaminant elimination in rats occurs mainly in the large intestine, Schlummer and colleagues [32] initially presumed that once the fat flush subsides, this fugacity gradient would result in diffusive elimination of chemical to feces in the lower digestive tract (similar to the MMD model). However, in later work, Moser and McLachlan [77] noted that the experimental evidence in the animal literature is inconsistent on this issue. For example, similar depuration studies in rats by Yoshimura and Yamamota [78] and Richter and Schafer [79] indicated that organism-to-intestine transfer of tetrachlorobiphenyl and hexachlorobenzene, respectively, occurs by passive diffusion in the upper intestine. In their assessment of the effects of a nonabsorbable fat substitute on human digestive elimination of POPs, Moser and McLachlan [80] concluded that chemical concentrations observed in the feces must be the result of an equilibration process within the intestinal tract because increasing the fugacity capacity of the feces increased the rate of chemical elimination. Furthermore, laboratory measurements indicated that the fugacity in human feces is considerably lower than the fugacity in the body [77]. This led to the conclusion that the fugacity gradient in the lower digestive tract does not result in significant chemical elimination, likely because of the absence of micelles in the lower digestive tract and hence slower mass transfer from the brush border into the lumen of the intestine [77,81]. Hence, the conclusion was made that the equilibration occurs in the upper gut.

McLachlan and colleagues [19,20,32,62,63,82,83] have conducted several investigations on intestinal absorption of various POPs in humans and agricultural food chains, with a focus on the bioavailability and intestinal absorption and de-

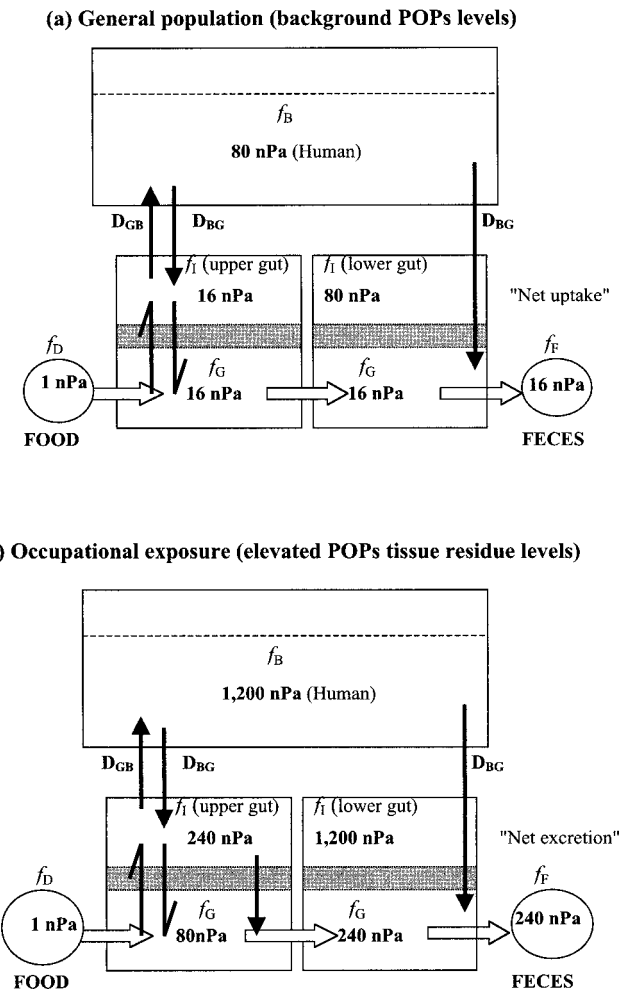

Fig. 8. Steady-state conditions of chemical fugacities in the gastrointestinal tract (GIT) and organism following the fat-flush diffusion model for (**a**) human subjects from the general population and (**b**) occupationally exposed persons. The GIT compartment (denoted as subscript G) is shown to include the intestinal wall (denoted as subscript I), separated by an unstirred water layer. POPs = persistent organic pollutants.

sorption kinetics of polychlorinated dioxins and furans. Studies involving human infants have shown that net dietary absorption efficiencies of most POPs are typically greater than 90% [83,84], whereas similar studies in adult human subjects show more variable results, ranging from high absorption efficiencies of 87% to instances of net excretion [32,63]. Studies by Schlummer et al. [32] and Rohde et al. [82] have shown that the net dietary absorption efficiency of a given compound in adult human subjects is highly dependent on the chemical concentration in blood lipids. If concentrations in blood lipids were comparable to levels in the background population, net contaminant absorption was generally observed. When observed concentrations in blood lipids were high compared to the background population (e.g., because of occupational exposure), net contaminant excretion was observed. Furthermore, the chemical elimination rate was linearly correlated with the concentration in the blood lipids. In fugacity terms, this implies that subjects excrete chemical if the blood-to-food fugacity (f_B/f_D) ratio is high, whereas net absorption typically occurs when fugacities in blood are low compared to food (i.e., low f_B/f_D ratios). Examination of these findings suggests that when tissue residue levels of a compound are high relative to the diet, efficient elimination occurs (likely due to a diffusive equilibration between the digesta and the wall of the upper digestive tract). This scenario is illustrated in Figure 8b, which shows a human subject who has approximately 15 times higher tissue residue levels compared to the general population (e.g., f_B = 1,200 nPa, perhaps due to occupational exposure) but consumes the same diet at 1 nPa (i.e., f_B/f_D = 1,200). In this case, the depression of the fugacity in the intestinal tissue (from 1,200 to 240 nPa) is not sufficient to bring it below the fugacity in the digesta (which rises to 80 nPa due to food digestion). Consequently, chemical moves along the diffusive gradient (from high fugacity in the body to low fugacity in the digesta) and net chemical excretion occurs until a partitioning equilibrium between the digesta and the intestinal tissue is achieved (i.e., f_D:f_G:f_I:f_B = 1:240:240:1,200).

The above evaluations of the fat-flush effect indicate that the intestine–digesta partition coefficient (K_{IG}) at the point of chemical absorption and desorption in the upper GIT is a critical parameter. The K_{IG} will largely be dependent on the respective volumes and fugacity capacities of those compartments (i.e., V_IZ_I vs V_GZ_G). Currently, the relative partitioning capacities and contaminant kinetics at the intestinal tissue–digesta interface are not fully understood. The question remains whether the dissociation of micelles at the gut wall (as described by the MMD model) precludes equilibrium of very hydrophobic POPs during chemical depuration back into the gut lumen. Specifically, further work is needed to resolve the issue of the disparity between D_{GB} and D_{BG}.

DISCUSSION

The review of the various proposed models on dietary absorption and biomagnification demonstrates that although some key differences exist, the models show a tendency to converge and build on each other and are not mutually exclusive. The digestion model demonstrates the role of food digestion on dietary absorption and magnification on the organism level. The FFD and MMD models describe how lipid digestion and absorption and chemical intestinal absorption and desorption are linked at the tissue level and alerts us to the possible existence of a magnification mechanism in addition to food digestion. The models combined provide a good theoretical framework for exploring the role of physicochemical properties on biomagnification that may be useful for chemical hazard assessment.

The key difference between the digestion and the MMD models concerns the role of micelles in transporting chemicals across gastrointestinal membranes. This particular part of the larger process of lipid absorption still remains unresolved. However, its use in models may have a significant impact on the selection of molecular descriptors for biomagnification. The MMD model predicts that BMF_{MAX} of a given compound is dependent on the chemical's K_{OW}, primarily because $D_{GB} > D_{BG}$. Specifically, the MMD model predicts that the BMF_{MAX} of nonmetabolizable compounds will be positively correlated with the chemical's K_{OW} because unidirectional micellar transport (and hence dietary uptake) enhances the rate if absorption for high-K_{OW} chemicals, whereas the reverse transport process from the organism to the gut lumen is reduced by an increase in K_{OW} (because of the absence of micelles in the lower GIT). Alternatively, the digestion model assumes that passive diffusion across the gut wall encounters similar diffusive restrictions during absorption and desorption (i.e., $D_{GB} = D_{BG}$) and indicates that the maximum bioaccumulation potential of com-

pounds (i.e., in absence of depuration via metabolism, urine excretion, and other mechanisms) is relatively universal and equivalent to $(G_D/G_F)(Z_D/Z_G)$, which is largely independent of K_{OW}. The FFD model can effectively compliment both the digestion or MMD model, depending on how intestinal desorption (organism-to-gut elimination) is envisioned. Currently, the influence of K_{OW} on the BMF_{MAX} in the FFD model is not fully understood and is essentially dependent on whether contaminant absorption and desorption are assumed to be decoupled processes or an equilibration in the upper GIT (i.e., $D_{GB} = D_{BG}$ vs $D_{GB} > D_{BG}$).

Regardless of the intestinal absorption–desorption mechanism, the BMF is ultimately the result of competing rates of chemical uptake from the GIT and other potential chemical elimination routes (i.e., respiration, urinary excretion, and metabolism), which are determined by a combination of organism physiology and the physicochemical properties of the compound. For aquatic poikilotherms, respiratory elimination makes a key contribution to the overall elimination of hydrophobic organic chemicals. Elimination to water (i.e., gill ventilation) has been repeatedly demonstrated to be inversely related to the chemical's K_{OW}. Hence, an increase in K_{OW} causes a slower rate of chemical elimination from the organism, allowing the fugacity in the organism to achieve levels that are closer to that in the GIT. For nonmetabolizable chemicals with K_{OW}s greater than 10^5, respiratory elimination is small compared to dietary elimination and biomagnification occurs. For air-breathing homeotherms, respiratory elimination is not to water but to the air. Respiratory elimination via lipid–air exchange declines with increasing octanol–air partition coefficient (K_{OA}), causing chemicals to approach a maximum biomagnification potential with increasing K_{OA}. The suggestion has been made that if K_{OA} exceeds 10^5, respiratory elimination is too small to effectively reduce the biomagnification effect in the GIT of many mammals, hence biomagnification can occur [42]. Only if the substance is rapidly eliminated to urine (e.g., log K_{OW} is less than ~2) or rapidly metabolized can biomagnification be prevented. Diminished BMFs due to metabolic transformation are more common in birds and mammals compared to fish, because those organisms generally have a greater capacity to metabolize organic contaminants [2,85,86]. The bioaccumulation potential of organic chemicals in aquatic organisms is best assessed by K_{OW}, whereas bioaccumulation potential in air-breathing organisms is best anticipated by K_{OA} and K_{OW} [42,43]. If K_{OW} and K_{OA} were to follow a simple single universal relationship among chemical classes, it would be possible to use K_{OW} alone as a predictor of biomagnification, but this is not the case [42,43,87]. Based on their K_{OW} and K_{OA}, chemicals can be categorized in four groups: polar nonvolatiles, nonpolar nonvolatiles, nonpolar volatiles, or polar volatiles. Figure 9 illustrates this categorization by using a limited number of chemicals for which bioaccumulation properties are relatively well known. Polar volatiles (bottom left quadrant) include compounds such as styrene and vinyl chloride and have no inherent bioaccumulative properties in either air-breathing or aquatic organisms. The nonpolar nonvolatiles (top right quadrant) represent the majority of POPs such as PCBs and several organochlorine pesticides (e.g., mirex) and are inherently bioaccumulative in both aquatic and air-breathing organisms. The polar nonvolatiles (top left quadrant) do not biomagnify in aquatic organisms (because of a low K_{OW}), but may substantially biomagnify in air-breathing organisms (because of a high K_{OA}) unless they are efficiently metabolized

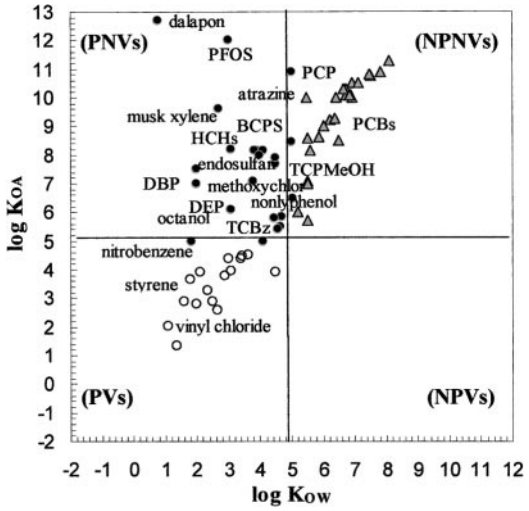

Fig. 9. Plot of log K_{OW} versus log K_{OA} for various organic chemicals, characterized into four quadrants: polar nonvolatiles (PNVs), nonpolar nonvolatiles (NPNVs), polar volatiles (PVs), and nonpolar volatiles (NPVs). BCPS = *bis*(4-chlorophenyl) sulfone; DBP = di-*n*-butyl phthalate; DEP = diethyl phthalate; HCHs = hexachlorocyclohexanes; PCB = polychlorinated biphenyl; PCP = pentachlorophenol; PFOS = perfluorooctane sulfonate; TCBz = trichlorobenzene; TCPMeOH = *tris*(4-chlorophenyl) methanol.

at a significantly high rate or depurated by urinary excretion. Examples of these relatively hydrophilic compounds exhibiting some degree of bioaccumulation potential include hexachlorocyclohexanes, endosulfan, atrazine, bis-4-chlorophenyl sulfone, trischlorophenyl methanol, and perfluorooctane sulfonate. Figure 9 shows no existing compounds with nonpolar volatile characteristics (bottom right). This group of chemicals may be quite rare, but theoretically involves chemicals with an inherent potential to biomagnify in water-respiring organisms but not in air-breathing organisms.

We believe that current regulatory initiatives aimed to identify bioaccumulative substances do not fully recognize some of the fundamental processes controlling biomagnification in air-breathing homeotherms and aquatic poikilotherms. This is a serious shortcoming of current regulatory initiatives because the bioaccumulative properties of many commercial chemicals may be misassessed or underestimated. This review demonstrates that significant evidence is available from theory (highlighted in this paper) and practice to indicate that BMFs in homeotherms cannot only be higher than those in aquatic organisms but also follow different relationships with the physicochemical properties of chemicals. Considering that the persistence, bioaccumulation, and inherent toxicity regulations are primarily geared to protect human health, this is a matter of some priority. Further investigations into the mechanism of bioaccumulation in homeotherms is important, as is research on the parameterization of bioaccumulation models. Measurements of feeding rates; chemical and lipid absorption efficiencies; the disparity between gastrointestinal transport parameters D_{GB} and D_{BG}; intestine–digesta partition coefficient (K_{IG}); fugacity capacities of food, digesta, and fecal matter; digesta transit times; and steady-state fugacity ratios between food, digesta, feces, and organism (i.e., f_D: f_G: f_F: f_B) are likely to be of crucial importance in this endeavor.

REFERENCES

1. Woodwell GM. 1967. Toxic substances and ecological cycles. *Sci Am* 216:24–31.

2. Muir DCG, Norstrom RJ, Simon M. 1988. Organochlorine contaminants in Arctic marine food chains: Accumulation of specific polychlorinated biphenyls and chlordane-related compounds. *Environ Sci Technol* 22:1071–1079.
3. Norstrom RJ, Simon M, Muir DCG. 1988. Organochlorine contaminants in Arctic marine food chains: Identification, geographical distribution, and temporal trends in polar bears. *Environ Sci Technol* 32:1063–1071.
4. Oliver BG, Niimi AJ. 1988. Trophodynamic analysis of polychlorinated biphenyl congeners and other chlorinated hydrocarbons in the Lake Ontario ecosystem. *Environ Sci Technol* 22: 390–396.
5. Borga K, Gabrielsen GW, Skaare JU. 2001. Biomagnification of organochlorines along a Barents Sea food chain. *Environ Pollut* 113:187–198.
6. Fisk AT, Hobson KA, Norstrom RJ. 2001. Influence of chemical and biological factors on trophic transfer of persistent organic pollutants in the northwater polynya marine food web. *Environ Sci Technol* 35:732–738.
7. Kelly BC, Gobas FAPC. 2001. Bioaccumulation of persistent organic pollutants in lichen–caribou–wolf food-chains of Canada's central and western Arctic. *Environ Sci Technol* 35:325–334.
8. Ratcliffe DA. 1967. Decrease in eggshell weight in certain birds of prey. *Nature* 215:208–210.
9. Paterson S, Mackay D. 1989. A model illustrating the environmental fate, exposure, and human uptake of persistent organic chemicals. *Ecol Model* 47:85–114.
10. Ross PS, Ellis GM, Ikonomou MG, Barrett-Lennard LG, Addison RF. 2000. High PCB concentrations in free ranging killer whales (*Orcinus orca*): Effects of age, sex, and dietary preference. *Mar Pollut Bull* 40:504–515.
11. Woodwell GM. 1984. Broken eggshells: The miracle of DDT was short-lived, but it helped launch the environmental movement. *Science* 84:115–117.
12. United Nations Environment Program. 1998. *Stockholm Treaty on POPs*. Stockholm, Sweden.
13. Gobas FAPC, Muir DCG, Mackay D. 1988. Dynamics of dietary bioaccumulation and fecal elimination of hydrophobic organic chemicals in fish. *Chemosphere* 17:943–962.
14. Gobas FAPC. 1993. A model for predicting the bioaccumulation of hydrophobic organic chemicals in aquatic food-webs: Application to Lake Ontario. *Ecol Model* 69:1–17.
15. Morrison HA, Gobas FAPC, Lazar R, Whittle M, Haffner GD. 1997. Development and verification of a benthic/pelagic food web bioaccumulation model for PCB congeners in western Lake Erie. *Environ Sci Technol* 31:3267–3273.
16. Fisk AT, Norstrom RJ, Cymbalisty CD, Muir DCG. 1998. Dietary accumulation and depuration of hydrophobic organochlorines: Bioaccumulation parameters and their relationships with the octanol–water partition coefficient. *Environ Toxicol Chem* 17:951–961.
17. Gobas FAPC, Zhang X, Wells R. 1993. Gastro-intestinal magnification: The mechanism of biomagnification and food-chain accumulation of organic chemicals. *Environ Sci Technol* 27: 2855–2863.
18. Campfens J, Mackay D. 1997. Fugacity-based model of PCB bioaccumulation in complex aquatic food webs. *Environ Sci Technol* 31:577–583.
19. McLachlan MS. 1994. Model of the fate of hydrophobic contaminants in cows. *Environ Sci Technol* 28:2407–2414.
20. McLachlan MS. 1996. Bioaccumulation of hydrophobic organic contaminants in agricultural food-chains. *Environ Sci Technol* 30:252–259.
21. Hendriks AJ, Ma WC, Brouns JJ, de Ruiter-Dijkman EM, Gast R. 1995. Modelling and monitoring organochlorine and heavy metal accumulation in soils, earthworms, and shrews in Rhine-delta floodplains. *Arch Environ Contam Toxicol* 29:115–127.
22. Norstrom RJ, Hallett DJ, Sonstegard RA. 1978. Coho salmon (*Oncorhynchus kisutch*) and herring gulls (*Larus argentatus*) as indicators of organochlorine contamination in Lake Ontario. *J Fish Res Board Can* 35:1401–1406.
23. Braune BM, Norstrom RJ. 1989. Dynamics of organochlorine compounds in herring gulls: III. Tissue distribution and bioaccumulation in Lake Ontario gulls. *Environ Toxicol Chem* 8:957–968.
24. Albanis TA, Hela D, Papakostas G, Goutner V. 1996. Concentration and bioaccumulation of organochlorine pesticide residues in herons and their prey in wetlands of Thermaikos Gulf, Macedonia, Greece. *Sci Total Environ* 182:11–19.
25. Leonards PEG, Broekhuizen S, de Voogt P, Van Straalen NM, Brinkman UAT, Cofino WP, van Hattum B. 1998. Studies of bioaccumulation and biotransformation of PCBs in mustelids based on concentration and congener patterns in predators and prey. *Arch Environ Contam Toxicol* 35:654–665.
26. Arctic Monitoring and Assessment Programme. 1998. *Arctic Pollution Issues.* Oslo, Norway.
27. Marsili L, Gaggi C, Bortolotto A, Stanzani L, Franchi A, Renzoni A, Bacci E. 1995. Recalcitrant organochlorine compounds in captive bottlenose dolphins (*Tursiops truncatus*): Biomagnification or bioaccumulation? *Chemosphere* 31:3919–3932.
28. Aono S, Tanabe S, Fujise Y, Kata H, Tatsukawa R. 1997. Persistent organochlorines in minke whale (*Balaenoptera acutorostrata*) and their prey species from the Antarctic and the North Pacific. *Environ Pollut* 98:81–89.
29. Nakata H, Tanabe S, Tatsukawa R, Amano M, Miyazaki N, Petrov EA. 1990. Persistent organochlorine residues and their accumulation kinetics in Baikal seal (*Phoca sibirica*) from Lake Baikal, Russia. *Environ Sci Technol* 29:2877–2885.
30. Weisbrod AV, Shea D, Moore MJ, Stegeman JJ. 2000. Organochlorine exposure and bioaccumulation in the endangered northwest Atlantic right whale (*Eubalaena glacialis*) population. *Environ Toxicol Chem* 19:654–666.
31. Varanasi U, Stein JE, Tilbury KL, Meador JP, Sloan CA, Brown DW, Chan SL, Calambokidis J. 1993. Chemical contaminants in gray whales (*Eschrichtius robustus*) stranded in Alaska, Washington, and California, USA. Technical Report NMFS-NWFSC-11. National Oceanic and Atmospheric Administration, Seattle, WA, USA.
32. Schlummer MG, Moser GA, McLachlan MS. 1998. Digestive tract absorption of PCDD/Fs PCBs and HCB in humans: Mass balances and mechanistic considerations. *Toxicol Appl Pharmacol* 152:128–137.
33. Hop H, Borga K, Gabrielsen GW, Skaare JU. 2002. Food web magnification of persistent organic pollutants in poikilotherms and homeotherms from the Barents Sea. *Environ Sci Technol* 36: 2589–2597.
34. Bidleman TF, Muir DCG, Stern GA. 1999. Synopsis of research conducted under the 1998/1999 Northern Contaminants Program. Technical Report R71-19/76-1999E. Indian Affairs and Northern Development, Ottawa, ON, Canada.
35. Martin JW, Mabury SA, Solomon KR, Muir DCG. 2003. Dietary accumulation of perfluorinated acids in juvenille rainbow trout (*Onchorhynchus mykiss*). *Environ Toxicol Chem* 22:189–195.
36. Kannan K, Corsolini S, Falandysz J, Oehme G, Focardi S, Giesy JP. 2002. Perfluorooctanesulfonate and related fluorinated hydrocarbons in marine mammals, fishes, and birds from coasts of the Baltic and the Mediterranean seas. *Environ Sci Technol* 36:3210–3216.
37. Kannan K, Franson JC, Bowerman WW, Hansen KJ, Jones PD, Giesy JP. 2001. Perfluorooctane sulfonate in fish-eating water birds including bald eagles and albatrosses. *Environ Sci Technol* 35:3065–3070.
38. Taniyasu S, Kannan K, Horii Y, Hanari N, Yamashita N. 2003. A survey of perfluorooctane sulfonate and related perfluorinated organic compounds in water, fish, birds, and humans from Japan. *Environ Sci Technol* 37:2634–2639.
39. Giesy JP, Kannan K. 2001. Global distribution of perfluorooctane sulfonate in wildlife. *Environ Sci Technol* 35:1339–1342.
40. Hu W, Jones PD, Upham BL, Trosko JE, Lau C, Giesy JP. 2002. Inhibition of gap junctional intercellular communication by perfluorinated compounds in rat liver and dolphin kidney epithelial cell lines in vitro and Sprague-Dawley rats in vivo. *Toxicol Sci* 68:429–436.
41. Upham BL, Deocampo ND, Wurl B, Trosko JE. 1998. Inhibition of gap junctional intercellular communication by perfluorinated fatty acids is dependent on the chain length of the fluorinated tail. *Int J Cancer* 78:491–495.
42. Kelly BC, Gobas FAPC. 2003. An Arctic terrestrial food chain bioaccumulation model for persistent organic pollutants. *Environ Sci Technol* 37:2966–2974.
43. Gobas FAPC, Kelly BC, Arnot JA. 2003. Quantitative structure activity relationships for predicting the bioaccumulation of POPs in terrestrial food-webs. *QSAR Combinator Sci* 22:329–336.

44. Beek B. 2000. *Bioaccumulation: New Aspects and Developments.* Springer-Verlag, Heidelberg, Germany.
45. Mackay D. 1991. *Multimedia Environmental Fate Models: The Fugacity Approach.* Lewis, Boca Raton, FL, USA.
46. Clark TP, Clark KE, Paterson S, Norstrom RJ, Mackay D. 1988. Wildlife, fugacity, and modelling. *Environ Sci Technol* 22:120–128.
47. Sanford P. 1992. *Physiological Principles in Medicine: Digestive System Physiology.* Edward Arnold, London, UK.
48. Johnson LR. 1981. *Gastrointestinal Physiology.* Mosby, St. Louis, MO, USA.
49. Thomson ABR, Schoeller C, Keelan M, Smith L, Clandinin MT. 1993. Lipid absorption: Passing through the unstirred water layer, brush-border membrane, and beyond. *Can J Physiol Pharmacol* 71:531–555.
50. Mutsch B, Gains N, Hauser H. 1986. Interaction of intestinal brush border membrane vesicles with small unilamellar phospholipid vesicles. Exchange of lipids between membranes is mediated by collisional contact. *Biochemistry* 25:2134–2140.
51. Weber LP, Lanno RP. 2001. Effect of bile salts, lipid, and humic acids on absorption of benzo[*a*]pyrene by isolated channel catfish (*Ictalurus punctatus*) intestine segments. *Environ Toxicol Chem* 20:117–1124.
52. Dulfer WJ, Govers HAJ, Groten JP. 1998. Kinetics and conductivity parameters of uptake and transport of polychlorinated biphenyls in the Caco-2 intestinal cell line model. *Environ Toxicol Chem* 17:493–501.
53. Nichols JW, Larsen CP, McDonald ME, Niemi GJ, Ankley GT. 1995. Bioenergetics-based model for accumulation of polychlorinated biphenyls by nestling tree swallows, *Tachycineta bicolor*. *Environ Sci Technol* 29:604–612.
54. Leib WR, Stein WD. 1986. *Transport and Diffusion Across Cell Membranes.* Academic, New York, NY, USA.
55. Connolly JP, Pedersen CJ. 1988. A thermodynamic-based evaluation of organic chemical accumulation in aquatic organisms. *Environ Sci Technol* 22:99–103.
56. Clark KE, Gobas F, Mackay D. 1990. Model of organic chemical uptake and clearance by fish from food and water. *Environ Sci Technol* 24:1203–1213.
57. Cahill TM, Cousins I, Mackay D. 2003. Development and application of a generalized physiologically based pharmacokinetic model for multiple environmental contaminants. *Environ Toxicol Chem* 22:26–34.
58. Hickie BE, Mackay D, de Koning J. 1999. A lifetime pharmacokinetic model for hydrophobic contaminants in marine mammals. *Environ Toxicol Chem* 18:2622–2633.
59. Gobas FAPC, McCorquodale JR, Haffner GD. 1993. Intestinal absorption and biomagnification of organochlorines. *Environ Toxicol Chem* 12:567–576.
60. Gobas FAPC, Wilcockson JB, Russel RW, Haffner GD. 1999. Mechanism of biomagnification in fish under laboratory and field conditions. *Environ Sci Technol* 33:133–141.
61. Drouillard KG, Norstrom RJ. 2000. Dietary absorption efficiencies and toxicokinetics of polychlorinated biphenyls in ring doves following exposure to Aroclor mixtures. *Environ Toxicol Chem* 19:2707–2714.
62. McLachlan MS. 1993. Mass balance of polychlorinated biphenyls and other organochlorine compounds in a lactating cow. *J Agric Food Chem* 41:474–480.
63. Moser GA, McLachlan MS. 2001. The influence of dietary concentration on the absorption and excretion of persistent lipophilic organic pollutants in the human intestinal tract. *Chemosphere* 45: 201–211.
64. Drouillard KG, Norstrom RJ. 2003. The influence of diet properties and feeding rates on PCB toxicokinetics in the ring dove. *Arch Environ Contam Toxicol* 44:99–106.
65. Fraser AJ, Burkow IC, Wolkers H, Mackay D. 2002. Modelling biomagnification and metabolism of contaminants in harp seals of the Barents Sea. *Environ Toxicol Chem* 21:55–61.
66. Lee JS, Tanabe S, Umino H, Tatsukawa R, Loughlin TR, Calkins DC. 1996. Persistent organochlorines in Steller sea lion (*Eumetopias jubatus*) from the bulk of Alaska and the Bering Sea, 1976–1981. *Mar Pollut Bull* 32:535–544.
67. Rosen DAS, Trites AW. 2000. Digestive efficiency and dry-matter digestibility in Stellar sea lions fed herring, pollock, squid and salmon. *Can J Zool* 78:234–239.
68. Pocock DME, Vost A. 1974. DDT absorption and chylomicron transport in rat. *Lipids* 9:374–381.
69. Charman WN, Porter CJJ, Mithani S, Dressman JB. 1997. Physiochemical and physiological mechanisms for the effects of food on drug absorption: The role of lipids and pH. *J Pharm Sci* 86: 269–282.
70. Laher JM, Rigler MW, Vetter RD, Barrowman JA. 1984. Similar bioavailability and lymphatic transport of benzo[*a*]pyrene when administered to rats in different amounts of dietary fat. *J Lipid Res* 25:1337–1342.
71. Dulfer WJ, Groten JP, Govers HAJ. 1996. Effect of fatty acids and the aqueous diffusion barrier on the uptake and transport of polychlorinated biphenyls in Caco-2 cells. *J Lipid Res* 37:950–961.
72. Vetter RD, Carey MC, Patton J.S. 1985. Coassimilation of dietary fat and benzo[*a*]pyrene in the small intestine: An absorption model using the killifish. *J Lipid Res* 26:428–434.
73. Rees DE, Mandelstam P, Lowry JQ, Lipscomb H. 1971. A study of the mechanism of intestinal absorption of benzo[*a*]pyrene. *Biochim Biophys Acta* 225:96–107.
74. Dulfer WJ, Govers HAJ. 1995. Membrane–water partitioning of polychlorinated biphenyls in small unilamellar vesicles of four saturated phosphatidylcholines. *Environ Sci Technol* 29:2548–2554.
75. Gobas FAPC, Lahittete JM, Garofalo G, Shiu WY, Mackay D. 1988. A novel method for measuring membrane–water partition coefficients of hydrophobic organic chemicals: Comparison with 1-octanol–water partitioning. *J Pharm Sci* 77:265–272.
76. Rozman T, Scheufler E, Rozman K. 1985. Effect of partial jejunectomy and colectomy on the disposition of hexachlorobenzene in rats treated or not treated with hexadecane. *Toxicol App Pharmacol* 78:421–427.
77. Moser GA, McLachlan MS. 2002. Partitioning of polychlorinated biphenyls and hexachlorobenzene into human faeces. *Chemosphere* 46:449–457.
78. Yoshimura H, Yamamota HA. 1975. A novel route of excretion of 2,4,3′4′-tetrachlorobiphenyl in rats. *Bull Environ Contam Toxicol* 13:681–688.
79. Richter E, Schafer SG. 1981. Intestinal excretion of hexachlorobenzene. *Arch Toxicol* 47:233–239.
80. Moser GA, McLachlan MS. 1999. A nonabsorbable dietary fat substitute enhances elimination of persistent lipophilic contaminants in humans. *Chemosphere* 39:1513–1521.
81. Moser GA, McLachlan MS. 2002. Modelling digestive tract absorption and desorption of lipophilic organic contaminants in humans. *Environ Sci Technol* 36:3318–3325.
82. Rohde S, Moser GA, Päpke O, McLachlan MS. 1999. Clearance of PCDD/Fs via the gastrointestinal tract in occupationally exposed persons. *Chemosphere* 39:3397–3410.
83. McLachlan MS. 1993. Digestive tract absorption of polychlorinated dibenzo-*p*-dioxins, dibenzofurans, and biphenyls in a nursing infant. *Toxicol Appl Pharm* 123:68–72.
84. Jodicke B, Ende M, Helge H, Neuber D. 1992. Fecal excretion of PCDDs/PCDFs in a 3-month old breast fed infant. *Chemosphere* 25:1061–1065.
85. Norstrom RJ, Clark TP, Jeffrey DA, Won HT, Gilman AP. 1986. Dynamics of organochlorine compounds in herring gulls (*Larus argentatus*): I. Distribution and clearance of [^{14}C] DDE in free-living herring gulls. *Environ Toxicol Chem* 5:41–48.
86. Norstrom RJ, Muir DCG. 1994. Chlorinated hydrocarbon contaminants in Arctic marine mammals. *Sci Total Environ* 154:107–128.
87. Arnot JA, Gobas FAPC. 2003. A generic QSAR for assessing the bioaccumulation potential of organic chemicals in aquatic food webs. *QSAR Combin Sci* 22:337–345.